Computational Study of the Reactions between XO (X = Cl, Br, I) and Dimethyl Sulfide

Hasan Sayin and Michael L. McKee*

Department of Chemistry and Biochemistry, Auburn University, Auburn, Alabama 36849

Received: May 15, 2004; In Final Form: July 10, 2004

The rate constants for reaction of XO (X = Cl, Br, I) with dimethyl sulfide (DMS) have been computed at high levels of theory. Two reaction pathways were considered: (1) the oxygen-atom transfer (OAT) by XO (X = Cl, Br, I) to form X and dimethyl sulfoxide (DMSO) and (2) the abstraction of hydrogen by XO (X = Cl, Br, I) to form XOH and $MeSCH_2$. Both reactions proceed via the formation of a very weak XO−DMS complex which can be described by natural bond orbital (NBO) analysis as a two-center one-electron (2c−1e) interaction where two α-spin electrons occupy lone pair orbitals (one localized on the oxygen atom and the other localized on the sulfur atom) and a β-spin electron occupies a σ bonding orbital (β-bond). The calculated OAT reaction rates of ClO, BrO, and IO with DMS are 3.0×10^{-15} $cm^3 \cdot s^{-1}$, 8.7×10^{-13} $cm^3 \cdot s^{-1}$ and 1.5×10^{-11} $cm^3 \cdot s^{-1}$, respectively, at 298 K and 760 Torr. The abstraction pathway is less favored in the order ClO > BrO > IO with computed branching ratios (OAT/abstraction) of 2.7, 98, and 15 000, for ClO, BrO, and IO, respectively.

Introduction

Dimethyl sulfide (DMS) is the most important reduced sulfur compound in the troposphere where it plays a major role regulating the climate through formation of cloud condensation nuclei in the troposphere.[1] Therefore, it is of great importance to understand the mechanism of DMS atmospheric transformations.[2−4] Unfortunately, there are many uncertainties in understanding the eventual fate of DMS in the atmosphere because of the lack of understanding of the oxidation mechanism. DMS, which is naturally emitted by oceanic phytoplankton, can reach the troposphere and react with halogen monoxide radicals in the catalytic ozone loss cycle (eq 1).[5]

$$DMS + XO \rightarrow DMSO + X \quad (X = Cl, Br, I) \qquad (1a)$$

$$O_3 + X \rightarrow O_2 + XO \qquad (1b)$$

A better understanding of the reactions of XO with DMS will permit a quantitative assessment of the importance of these reactions in atmospheric models.

The experimental measurements of the reaction rates between XO and DMS (X = Cl, Br, I) are collected in Table 1.[6−16] While the hydrogen abstraction pathway is the major pathway in the reaction of Cl and NO_3 with DMS, this pathway does not appear to be important in the reaction of XO (X = Cl, Br, I) with DMS. Instead, only the oxygen-atom transfer (OAT) pathway is observed, with DMSO as the single product detected in high yield.

As seen from Table 1, there is fairly good agreement on rate constants of ClO and BrO reactions with DMS. On the other hand, the rate constant varies by almost 4 orders of magnitude for the IO + DMS reaction. At the slow end, the reaction would not be an important atmospheric loss process for DMS, while it would be on the fast end. One of the goals of the present study is to determine the rate constant for the IO + DMS reaction as accurately as possible.

From the experimental exothermicities[17] for the reactions of ClO, BrO, and IO with DMS to form Cl, Br, and I plus DMSO (-22.4 $kcal \cdot mol^{-1}$, -27.5 $kcal \cdot mol^{-1}$, and -29.0 $kcal \cdot mol^{-1}$, respectively), one would expect the reactivity order ClO < BrO < IO. The reactions of ClO and BrO follow this trend, but the variations in the rate constant determinations for the IO reaction are too large to determine whether the trend is followed.

We will consider two possible reaction pathways: (a) oxygen-atom transfer (OAT) from XO (X = Cl, Br, I) to DMS and (b) abstraction of hydrogen by XO (X = Cl, Br, I) (eqs 2, 3).

$$MeSCH_3 + XO \rightarrow MeS(O)CH_3 + X \qquad (2)$$

$$MeSCH_3 + XO \rightarrow MeSCH_2 + HOX \quad (X = Cl, Br, I) \qquad (3)$$

For X = Cl, an additional pathway is considered, the abstraction of hydrogen from DMSO by chlorine atom (eq 4) which is exothermic for X = Cl but

$$MeS(O)CH_3 + Cl \rightarrow MeS(O)CH_2 + HCl \qquad (4)$$

endothermic for X = Br and I.

Method

All calculations were made using the Gaussian 98 program[18] system. Optimization and frequency calculations were carried out at the B3LYP/6-311+G(d,p) level (X = Cl and Br) and B3LYP/6-311+G(d,p)/ECP (X = I). All imaginary frequencies for transition states were tested by using the graphical program (MOLDEN)[19] to make sure that the motion was appropriate for converting reactants to products. For X = Cl, G3B3[20] energies have been determined using B3LYP/6-31G(d) geometries. For X = Br and I, a series of single-point calculations (using B3LYP/6-311+G(d,p) or B3LYP/6-311+G(d,p)/ECP geometries) have been combined to form G2B3(MP2)[21,22] and G3B3(MP2)[23,24] energies with only slight deviations from the standard procedure. The G3B3(MP2) energies were not determined for X = I because the method has not been defined for the iodine atom.

10.1021/jp0479116 CCC: $27.50
Published on Web 08/21/2004

TABLE 1: Experimental and Theoretical Rate Constant ($cm^3 \cdot s^{-1}$) for XO + DMS (X = Cl, Br, I) at 298 K

	pressure (Torr)	exptl k	ref	calc k^a
ClO + DMS				
flow tube MS	1.8−5.1 (He)	$(9.5 \pm 2.0) \times 10^{-15}$	6	3.0×10^{-15}
flow tube MS	0.5−2	$(3.9 \pm 1.2) \times 10^{-15}$	7	
BrO + DMS[b]				
flow tube MS	1.8−5.1 (He)	$(2.7 \pm 0.5) \times 10^{-13}$	6	8.7×10^{-13}
flow tube MS		$(2.7 \pm 0.2) \times 10^{-13}$	8	
laser photolysis absorption	60−100 (N_2)	$(4.4 \pm 0.6) \times 10^{-13}$	9	
cavity ring down spectroscopy	100 (N_2)	4.2×10^{-13}	10	
IO + DMS				
smog chamber FTIR	760 (N_2)	$(3 \pm 1.5) \times 10^{-11}$	11	1.5×10^{-11}
flow tube MS	1 (Ne)	$(1.5 \pm 0.5) \times 10^{-11}$	12	
laser photolysis absorption	40−300 (N_2, O_2, air)	$<3.5 \times 10^{-14}$	13	
flow tube MS	1.58−5.1 (He)	$(8.8 \pm 2.1) \times 10^{-15}$	6	
flow tube MS	1.1−1.4 (He)	$(1.5 \pm 0.2) \times 10^{-14}$	14	
flow tube MS	2.5−2.7 (He)	$(1.6 \pm 0.1) \times 10^{-14}$	15	
cavity ring down spectroscopy	100 (N_2)	$(2.5 \pm 0.2) \times 10^{-13}$	16	

[a] This work. [b] The rate constant for the BrO + MeSH reaction at 298 K is 4.54×10^{-14} $cm^3 \cdot s^{-1}$. Aranda, A.; Díaz de Mera, Y.; Rodríguez, D.; Salgado, S.; Martínez, E. *Chem. Phys. Lett.* **2002**, *357*, 471.

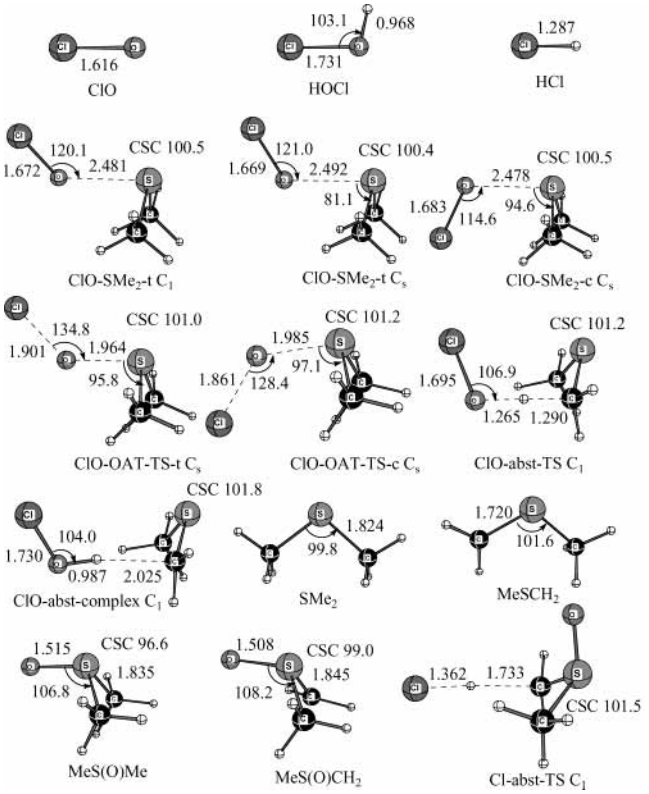

Figure 1. Optimized geometric parameters of stationary points at the B3LYP/6-311+G(d,p) level. Bond lengths are in angstroms and angles are in degrees. The optimized structure of Cl-abst-TS is at the MP2/6-31G(d) level.

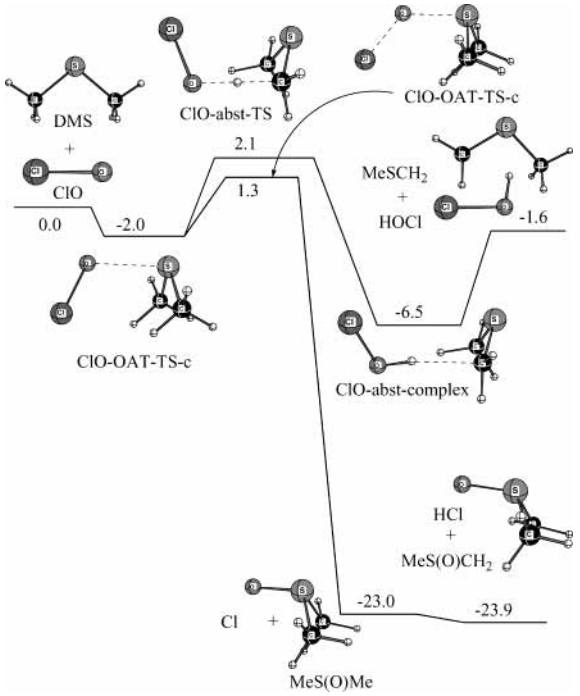

Figure 2. Reaction profile of enthalpies ($kcal \cdot mol^{-1}$) computed at the G3B3 (298 K) level for the reaction of ClO with DMS. Molecular plots are made from optimized Cartesian coordinates.

G2B3(MP2) theory corresponds effectively to calculations at the QCISD(T)/6-311+G(3df,2p) level with zero-point vibrational energies (ZPE) and higher-level corrections (HLC). The G2B3(MP2) method was extended by Radom and co-workers[22] to bromine- and iodine-containing compounds using basis sets which include effective core potentials (ECP)[25] and first-order spin−orbit corrections (SOC) for Br and I atoms. Recently, the G3B3(MP2) method has been extended to X = Br where all-electron basis sets are used on bromine.[24] In the calculations presented here (and a slight deviation from the standard G2B3-(MP2) and G3B3(MP2) methods), SOC will be included for X, XO, XO/DMS complexes and XO/OAT transition states (X = Cl, Br, I). The XO radicals have $^2\Pi$ ground states and are expected to have large SOCs. The XO/DMS complexes (and to a lesser extent XO/OAT transition states) have weak interactions between the XO radical and DMS such that the spin−orbital coupling effect may not be fully quenched.

The SOCs have been calculated for X, XO, XO/DMS complexes and XO/OAT transition states (X = Cl, Br, and I) and compared with other calculations and experiment in Table 2. The calculations used full Breit−Pauli spin−orbit coupling,[26] an all-electron 6-311G(d) basis set, and an active space that varied with the compound ((5e,3o), (13e,8o), and (15e,10o) for X, XO, and XO−DMS/XO-OAT-TS, respectively). The calculated and experimental SOCs are in reasonable agreement for X and XO (Table 2) which suggests that the XO−DMS/XO-OAT-TS SOCs may have similar accuracy. We have decided to use the experimental SOCs for X and XO and the calculated SOCs for XO−DMS/XO-OAT-TS. While the SOC for BrO and IO are large (0.92 and 1.99 $kcal \cdot mol^{-1}$, respectively) and should not be ignored, the SOCs for XO−DMS and XO-OAT-TS

TABLE 2: Spin−Orbit Corrections (SOC) in kcal·mol^{-1} [a]

	calculated		
	this work[b]	others	exptl
Cl	0.78	0.82[c]	0.84[d]
ClO	0.33	0.20,[e] 0.30,[f] 0.28[g]	0.30[h]
ClO−SMe_2-c C_s	0.01		
ClO-OAT-TS-c C_s	0.00		
Br	3.20	3.63[i]	3.51[d]
BrO	0.84	0.64,[e] 0.92,[i] 0.78[g]	0.92[j]
BrO−SMe_2-c C_s	0.05		
BrO-OAT-TS-c C_s	0.02		
I	6.55	7.02[k]	7.25[l]
IO	1.48	1.60,[k] 1.70,[e] 1.75[g]	1.99[m]
IO−SMe_2-c C_s	0.13		
IO-OAT-TS-c C_s	0.08		

[a] The spin−orbit correction (SOC) is the difference between the lowest spin−orbit coupled state and the *J*-averaged state. For the ^{2}P and $^2\Pi$ electronic states of X and XO (X = Cl, Br, I), respectively, the SOC is $\lambda/2$ where λ is the spin−orbit coupling constant (SOCC). Equivalently, the SOC is $^1/_3$ of the fine structure splitting (FSS) where FSS = $\Delta(^2P_{1/2} - {}^2P_{3/2})$ for X and FSS = $\Delta(^2\Pi_{1/2} - {}^2\Pi_{3/2})$ for XO, respectively. [b] The GAMESS program was used to calculated the full Breit−Pauli spin−orbit coupling[26] with a (5e,3o), (13e,8o), and (15e,10o) active space for X, XO, and XO−SMe_2, respectively, and a 6-311G(d) all-electron basis set. GAMESS: Schmidt, M. W.; Baldridge, K. K.; Boatz, J. A.; Elbert, S. T.; Gordon, M. S.; Jensen, J. J.; Koseki, S.; Matsunaga, N.; Nguyen, K. A.; Su, S.; Windus, T. L.; Dupuis, M.; Montgomery J. A. *J. Comput. Chem.* **1993**, *14*, 1347. All-electron 6-311G(d) basis set: Krishnan, R.; Binkley, J. S.; Seeger, R.; Pople, J. A. *J. Chem. Phys.* **1980**, *72*, 650. McLean, A. D.; Chandler, G. S. *J. Chem. Phys.* **1980**, *72*, 5639. Blaudeau, J.-P.; McGrath, M. P.; Curtiss, L. A.; Radom, L. *J. Chem. Phys.* **1997**, *107*, 5016. Curtiss, L. A.; McGrath, M. P.; Blandeau, J. P.; Davis, N. E.; Binning, R. C., Jr.; Radom, L. *J. Chem. Phys.* **1995**, *103*, 6104. Glukhovstev, M. N.; Pross, A.; McGrath, M. P.; Radom, L. *J. Chem. Phys.* **1995**, *103*, 1878. [c] Iliaš, M.; Kellö, V.; Visscher, L.; Schimmelpfenning, B. *J. Chem. Phys.* **2001**, *115*, 9667. [d] Moore, C. E. *Atomic Energy Levels*; NSRDS-NBS 35; National Bureau of Standards: Washington, DC, 1971; Vol. I−III.[e] Ma, N. L.; Cheung, Y.-S.; Ng, C. Y.; Li, W.-K. *Mol. Phys.* **1997**, *91*, 495. [f] Berning, A.; Schwqeizer, M.; Werner, H.-J.; Knowles, P. J.; Palmieri, P. *Mol. Phys.* **2000**, *98*, 1823. [g] Koseki, S.; Gordon, M. S.; Schmidt, M. W.; Matsunaga, N. *J. Phys. Chem.* **1995**, *99*, 12764. [h] Coxon, J. A. *Can. J. Phys.* **1979**, *57*, 1538. [i] Bladeau, J.-P.; Curtiss, L. A. *Int. J. Quantum Chem.* **1997**, *61*, 943. [j] McKellar, A. R. W. *J. Mol. Spectrosc.* **1981**, *86*, 43. [k] Roszak, S.; Krauss, M.; Alekseyev, A. B.; Liebermann, H.-P.; Buenker, R. J. *J. Phys. Chem. A* **2000**, *104*, 2999. [l] Lias, S. G.; Bartmass, J. E.; Liebman, J. F.; Holmes, J. L.; Levin, R. D.; Mallard, W. G. *J. Phys. Chem. Ref. Data* **1988**, *17*, (Suppl. No. 1). [m] Gilles, M. K.; Polak, M. L.; Lineberger, W. C. *J. Chem. Phys.* **1991**, *95*, 4723.

species are all less than 0.13 kcal·mol^{-1} and could probably be ignored. Morokuma and co-workers[27] have computed SOCs at a similar level of theory for reactions including IO + $C_2H_5 \rightarrow$ HOI + C_2H_4 at the G2M(RCC) level and have obtained similar corrections.

Calculated total energies, zero-point energies, heat capacity corrections, and entropies are given as Supporting Information (Table S1) while relative energies (and related thermodynamic properties) are given in Table 3. Since the relative energies for Br-containing species at the G2B3(MP2) and G3B3(MP2) levels are very similar (Table S2), we will only discuss relative energies at the G3B3(MP2) level for X = Br. The structures and enthalpies of species on the XO−DMS PES are given for ClO−DMS in Figures 1 and 2, for BrO−DMS in Figures 3 and 4 and for IO−DMS in Figures 5 and 6.

Rate constants were calculated by using the CHEMRATE software package.[28] Vibrational frequencies and structures were calculated at the B3LYP/6-311+G(d,p) level for X = Cl and Br and at B3LYP/6-311+G(d,p)/ECP for X = I and used as input along with energies at the G3B3, G3B3(MP2), and G2B3-

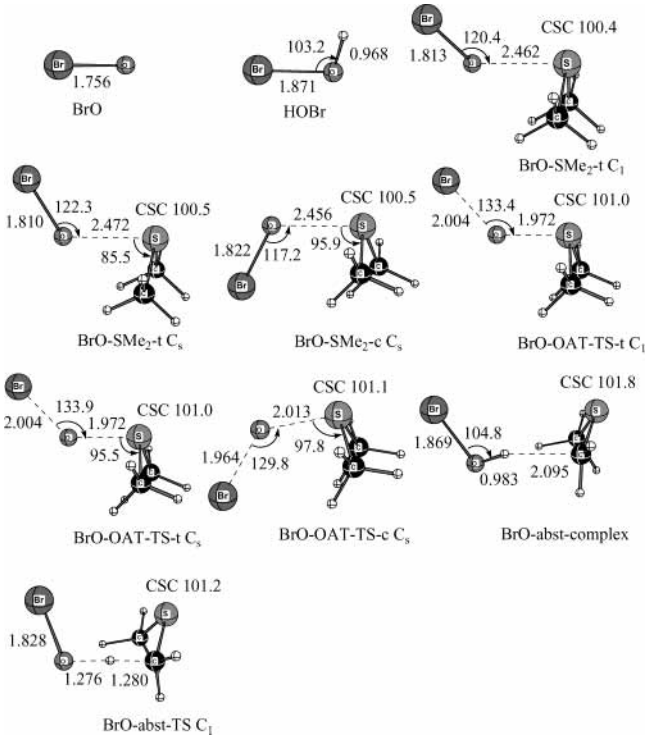

Figure 3. Optimized geometric parameters of stationary points at the B3LYP/6-311+G(d,p) level. Bond lengths are in angstroms and angles are in degrees.

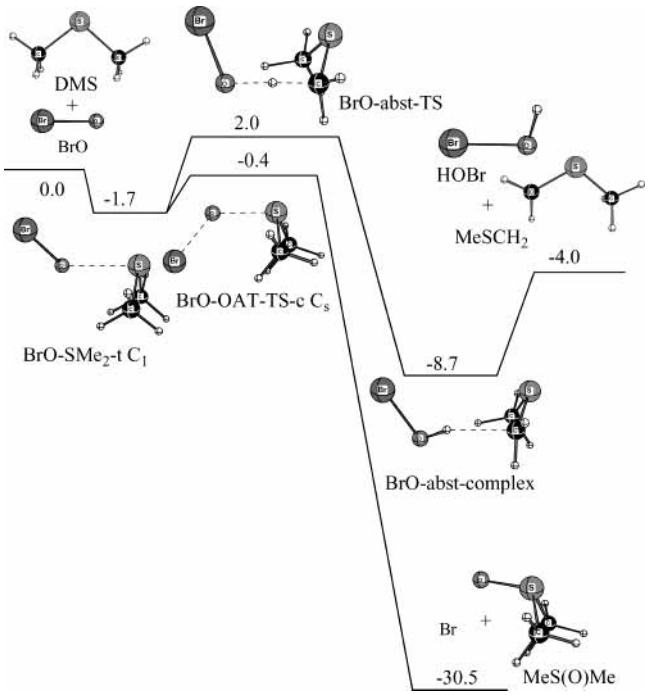

Figure 4. Reaction profile of enthalpies (kcal·mol^{-1}) computed at the G3B3(MP2) (298 K) level for the reaction of BrO with DMS.

(MP2) levels for X = Cl, Br, and I, respectively. The normal modes corresponding to methyl and XO rotation were treated as torsions rather as vibrations, and the experimental spin−orbit splitting of XO was included as input to the CHEMRATE program.

Natural bond orbital (NBO) analysis[29] was done at the B3LYP/6-311+G(d,p) level for X = Cl and Br and at the B3LYP/6-311+G(d,p)/ECP level for X = I to understand the nature of bonding in the XO−DMS complexes.

TABLE 3: Relative Energies (kcal·mol^{-1}) at the DFT and ab Initio Levels for Various Species Involved in the XO + DMS Reactions (X = Cl, Br, I)

	B3LYP/6-311+G(d,p)				ab initio[a]			
	E_e	ΔH (0 K)	ΔH (298 K)	ΔG (298 K)	ΔH (0 K)	ΔH (0 K) + SOC	ΔH (298 K)	ΔG (298 K)
ClO + DMS	0.0	0.0	0.0	0.0	0.0	0.0	0.0	0.0
ClO−SMe_2-t C_1	−7.2	−6.3	−6.1	2.1	−1.6	−1.4	−1.2	7.1
ClO−SMe_2-t C_s	−7.1	−6.3	−6.7	3.2	−1.5	−1.3	−1.6	8.3
ClO−SMe_2-c C_s	−6.1	−5.3	−5.2	3.3	−1.8	−1.6	−2.0	6.5
ClO-abst-complex	−5.2	−5.4	−5.0	1.6	−7.0	−6.8	−6.5	0.1
ClO-OAT-TS-t C_s	1.4	1.7	1.5	10.8	7.2	7.4	7.3	16.6
ClO-OAT-TS-c C_s	−1.5	−1.0	−1.1	8.9	1.5	1.7	1.3	11.3
ClO-abst-TS	2.4	−0.2	−0.6	8.5	2.3	2.5	2.1	11.2
MeS(O)Me + Cl	−12.8	−11.8	−12.0	−8.8	−22.2	−22.8	−23.0	−19.8
$MeSCH_2$ + HOCl	0.5	−1.6	−0.9	−3.7	−2.2	−12.0	−1.6	−4.3
$MeS(O)CH_2$ + HCl	−9.3	−12.9	−12.4	−11.7	−24.7	−24.5	−23.9	−23.2
Cl-abst-TS[b]	−12.1	−14.3	−15.0	−4.7	−23.3	−22.9	−23.8	−13.4
BrO + DMS	0.0	0.0	0.0	0.0	0.0	0.0	0.0	0.0
BrO−SMe_2-t C_1	−6.8	−6.3	−6.1	2.1	−2.8	−1.9	−1.7	6.5
BrO−SMe_2-t C_s	−6.8	−6.4	−6.1	1.9	−2.5	−1.6	−1.4	6.6
BrO−SMe_2-c C_s	−5.4	−5.0	−4.8	3.4	−2.8	−1.9	−1.7	6.5
BrO-abst-complex	−6.4	−6.9	−6.5	0.8	−10.0	−9.1	−8.7	−1.4
BrO-OAT-TS-t C_1	−0.7	−0.6	−0.8	8.7	3.2	4.1	3.9	13.4
BrO-OAT-TS-t C_s	−0.7	−0.7	−1.4	9.5	3.1	4.0	3.4	14.2
BrO-OAT-TS-c C_s	−2.7	−2.5	−2.8	7.1	−1.1	−0.2	−0.4	9.4
BrO-abst-TS	1.9	−1.0	−1.3	8.1	1.3	2.3	2.0	11.4
MeS(O)Me + Br	−15.9	−15.0	−15.2	−11.9	−27.7	−30.3	−30.5	−27.2
$MeSCH_2$ + HOBr	−1.2	−3.7	−3.0	−5.7	−5.6	−4.7	−4.0	−6.7
IO + DMS	0.0	0.0	0.0	0.0	0.0	0.0	0.0	0.0
IO−SMe_2-t C_1	−8.9	−8.0	−7.8	0.4	−3.4	−1.5	−1.3	6.9
IO−SMe_2-t C_s	−8.7	−7.9	−7.7	−0.3	−2.6	−0.8	−0.5	6.8
IO−SMe_2-c C_s	−6.6	−6.0	−5.7	2.5	−2.2	−0.4	−0.1	8.1
IO-abst-complex	−10.9	−11.2	−10.8	−3.8	−13.3	−11.4	−10.9	−4.0
IO-OAT-TS-t C_1	−6.8	−6.3	−6.4	2.6	−1.1	0.8	0.7	9.8
IO-OAT-TS-t C_s	−6.7	−6.4	−7.0	3.8	−1.6	0.4	−0.3	10.6
IO-OAT-TS-c C_s	−6.6	−6.0	−6.2	3.3	−4.4	−2.4	−2.6	6.9
IO-abst-TS	−0.3	−2.8	−3.1	5.9	1.6	3.6	3.3	12.3
MeS(O)Me + I	−25.8	−24.4	−24.6	−21.3	−32.9	−38.1	−38.3	−35.0
$MeSCH_2$ + HOI	−5.3	−7.7	−7.0	−9.8	−8.5	−6.5	−5.8	−8.6

[a] The values for ClO + DMS, BrO + DMS, IO + DMS at the ab initio level are calculated by using G3B3, G3B3(MP2), and G2B3(MP2) methods, respectively. The G3 methods include SOC for atoms heavier than Ne. The entries under ΔH (0 K) have this correction subtracted. The entries under ΔH (0 K) + SOC have SOC added for X and XO as well as the XO/DMS complexes and OAT transition states. The SOC of X and XO are from experiment and the SOC of XO−SMe_2-c (C_s) and XO-OAT-TS-c (C_s) are from calculations. The SOC of XO−SMe_2-t and XO-OAT-TS-t (trans orientation) was assumed to be the same as the corresponding cis structure. The thermodynamic properties are obtained from unscaled vibrational frequencies. [b] The transition state "Cl-abst-TS" was located at the MP2/6-31G(d) level because the structure could not be located at the DFT level. Further calculations (DFT and ab initio) were made on this geometry.

Results and Discussion

ClO + DMS. Two orientations of ClO with DMS were considered, cis and trans. At the B3LYP/6-311+G(d,p) level, the trans ClO−DMS complex (C_s complex) was 1.0 kcal·mol^{-1} more stable than the cis complex. The C_s trans complex had one imaginary frequency at the B3LYP/6-311+G(d,p) level and led to a C_1 minimum, 0.1 kcal·mol^{-1} lower in energy. At the G3B3 level, the cis complex was 0.2 kcal·mol^{-1} lower in energy than the trans complex (0.8 kcal·mol^{-1} lower with SOC at 298 K). In addition, the binding enthalpy of the complex is much smaller at the G3B3 level (2.0 kcal·mol^{-1}) compared to DFT (6.7 kcal·mol^{-1}).

The oxygen-atom transfer (OAT) transition states were also computed in the cis and trans orientations where the former was lower in enthalpy than the latter by 6.0 kcal·mol^{-1} (G3B3, Table 3). While the structures of the two transition states (ClO-OAT-TS-c and ClO-OAT-TS-t) are similar, the cis TS is earlier than the trans as judged by the longer S−O distance (1.985 compared to 1.964 Å) and the shorter Cl−O distance (1.861 compared to 1.901 Å), which is consistent with the smaller activation enthalpy (3.3 compared to 8.9 kcal·mol^{-1}). The lower enthalpy of the cis TS (relative to the trans TS) is due to the favorable electrostatic interaction of the ClO unit with the methyl hydrogens of DMS. The cis TS is also favored in XO-OAT-TS (X = Br and I) for the same reason, but the difference decreases from 6.0 kcal·mol^{-1} for X = Cl to 3.8 and 2.3 kcal·mol^{-1} for X = Br and I, respectively.

The initial product of the OAT reaction is Cl + DMSO which is calculated to be 23.0 kcal·mol^{-1} more stable than ClO + DMS (22.4 kcal·mol^{-1}, exptl). However, the calculated bond dissociation enthalpy of Cl−H and $MeS(O)CH_2$−H are 103.0 kcal·mol^{-1} and 98.5 kcal·mol^{-1}, respectively, which indicates that the Cl radical can exothermically abstract a hydrogen from DMSO to form HCl + $MeS(O)CH_2$. The transition state geometry for the abstraction was taken from MP2/6-31G(d) because the transition state could not be located at the B3LYP/6-31G(d) or B3LYP/6-311+G(d,p) levels. The enthalpy of Cl-abst-TS at G3B3 (using the MP2/6-31G(d) geometry) was 0.8 kcal·mol^{-1} below Cl + DMSO. On the other hand, the free energy of Cl-abst-TS is 6.4 kcal·mol^{-1} higher than Cl + DMSO at 298 K. Very similar results have been obtained by Vandresen et al.[30] where values of $\Delta H^{\ddagger} = -2.5$ kcal·mol^{-1} and $\Delta G^{\ddagger} = 4.6$ kcal·mol^{-1} were obtained.

In the abstraction transition state (ClO-abst-TS), the forming O−H bond is 1.265 Å and the breaking C−H bond is 1.290 Å. A hydrogen-bonded complex is formed (ClO-abst-complex) which is bound by 4.9 kcal·mol^{-1} relative to HOCl + $MeSCH_2$. The small difference between the ClO-OAT-TS and the abstrac-

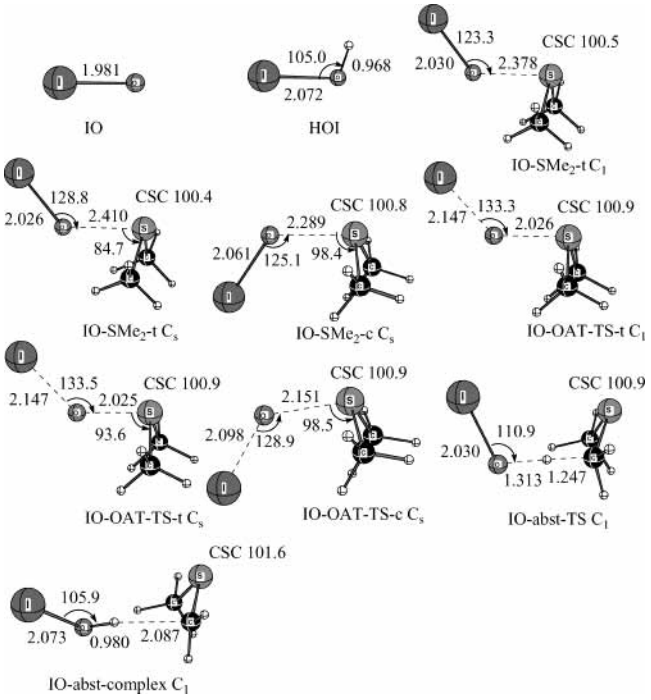

Figure 5. Optimized geometric parameters of stationary points at the B3LYP/6-311+G(d,p)/ECP level. Bond lengths are in angstroms and angles are in degrees.

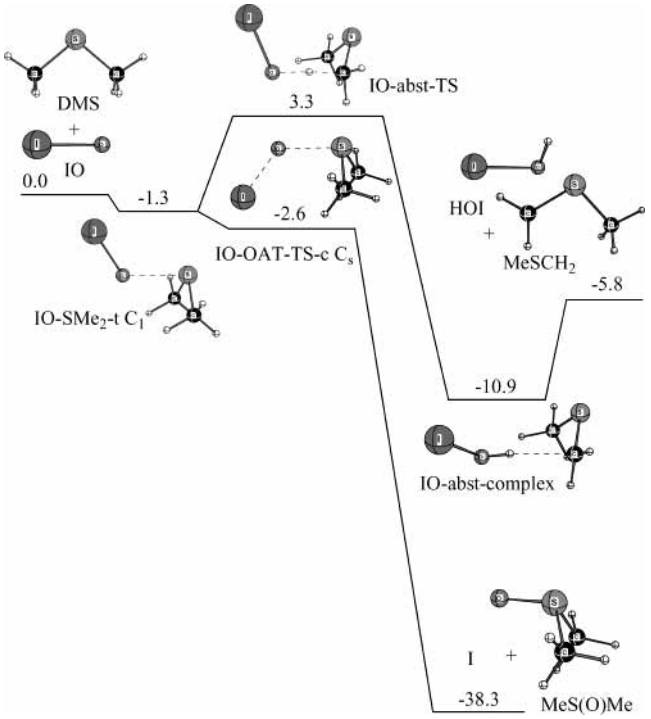

Figure 6. Reaction profile of enthalpies (kcal·mol^{-1}) computed at the G2B3(MP2) (298 K) level for the reaction of IO with DMS.

tion barriers (1.3 compared to 2.1 kcal·mol^{-1}) suggests that products from both pathways should be observed. However, the HOCl/$MeSCH_2$ products have not been reported from experiments.[6,7] In contrast to experimental results on the reaction between ClO + DMS, Stickel et al.[31] and Butkovskaya et al.[32] report that hydrogen abstraction is the dominant reaction pathway at low pressure in the reaction between Cl + DMS. We note that the rate of H-abstraction from DMS by Cl is much faster than the rate of OAT from ClO to DMS $(3.3 \pm 0.5) \times 10^{-10}$ compared to $(3.9 \pm 1.2) \times 10^{-15}$ cm^3·s^{-1} at 298 K (Table 1).

There are two ways to compute the rate constant: (1) as a bimolecular reaction with ClO and DMS as reactants and (2) as a unimolecular pathway with the ClO−DMS complex as reactant. In the first scenario, the A-factor will be less favorable but the activation energy will be smaller, while in the second scenario, the A-factor will be more favorable but the activation energy will be larger. In the unimolecular case, the rate constant was computed as $k = K_5 \cdot k_6$ where k_6 is obtained from CHEMRATE (eq 6) and K_5 is obtained from $\Delta G = -RT \ln K_5$ using the calculated free energy change of eq 5.

$$\mathrm{ClO} + \mathrm{DMS} \rightarrow \mathrm{ClO{-}DMS} \quad (5)$$

$$\mathrm{ClO{-}DMS} \rightarrow \mathrm{Cl} + \mathrm{DMSO} \quad (6)$$

In the ClO + DMS reaction, the computed bimolecular rate constant was much faster than K_5 times the unimolecular rate constant (k_6). Thus, the enthalpy of binding of the ClO−DMS complex does not compensate for unfavorable entropy of binding and leads to K_5 much smaller than 1. Only the bimolecular rate constant is reported.

The calculated rate constant for the OAT pathway and abstraction pathway are 3.0×10^{-15} and 1.1×10^{-15} cm^3·s^{-1}, respectively, at 298 K and 760 Torr; the branching ratio is 2.7 favoring the OAT pathway. The computed rate constant for the ClO + DMS reaction is in good agreement with experiment (Table 1).

BrO + DMS. The initial complex between BrO and DMS is 1.7 kcal·mol^{-1} more stable than the separated reactants and nearly equally stable in the cis and trans orientation. The nonbonded Br···H distance is 3.140 Å in the cis isomer (BrO−SMe_2-c), close to the sum of the van der Waals (vdW) radii of Br (1.97 Å)[33a] and H (1.10 Å)[33b] which may indicate some interaction. In the corresponding ClO complex (ClO−SMe_2-c), the nonbonding Cl···H distance is 2.894 Å, somewhat smaller than the sum of the vdW radii between chloride (1.90 Å)[33a] and hydrogen (1.10 Å). The transition state for OAT is 3.8 kcal·mol^{-1} lower in the cis than in the trans orientation due to more favorable electrostatic interactions in the former. Consistent with the smaller activation enthalpy, the cis OAT TS is earlier than the trans TS as judged by the longer forming S−O bond (2.013 compared to 1.972 Å) and the shorter breaking Br−O bond (1.964 compared to 2.004 Å). The activation enthalpy for the OAT pathway is negative with respect to separated reactants (−0.4 kcal·mol^{-1}) while the free energy of activation is 9.4 kcal·mol^{-1}. For comparison, Bedjanian et al.[8] and Nakano et al.[10] have determined negative activation energies of -2.1 ± 0.5 kcal·mol^{-1} and -1.7 ± 0.5 kcal·mol^{-1}, respectively, for this reaction.

The products, Br + DMSO, are calculated to be 30.5 kcal·mol^{-1} exothermic which can be compared to the experimental value[17] of 27.5 kcal·mol^{-1}. The Br radical is not expected to abstract a hydrogen from DMSO because the calculated Br−H bond enthalpy in HBr (86.9 kcal·mol^{-1}) is smaller than the calculated C−H bond enthalpy in DMSO (98.5 kcal·mol^{-1}).

The abstraction transition state is 2.4 kcal·mol^{-1} higher in enthalpy than the OAT transition state, consistent with the experimental results that the abstraction pathway is not observed.[6,8−10] The calculated rate constant[34] for the OAT and hydrogen abstraction pathways are 8.7×10^{-13} cm^3·s^{-1} and 8.9×10^{-15} cm^3·s^{-1}, respectively, at 298 K and 760 Torr which gives a branching ratio of 98. The calculated rate constant for the OAT pathway (8.7×10^{-13} cm^3·s^{-1}) is in good agreement with experiment ($(3 \pm 1) \times 10^{-13}$ cm^3·s^{-1}).

IO + DMS. The trans IO−DMS complex (IO−SMe_2-t C_1) is more stable than the cis complex (IO−SMe_2-c C_s) by 1.2

TABLE 4: Calculated Rate Constants ($cm^3 \cdot s^{-1}$) and Branching Ratios of XO + DMS (X = Cl, Br, I) at 298 K for Oxygen-Atom Transfer (OAT) and Hydrogen Abstraction Pathways

	OAT (k_1)	abstraction (k_2)	branching ratio (k_1/k_2)
ClO + DMS	3.0×10^{-15}	1.1×10^{-15}	2.7
BrO + DMS	8.7×10^{-13}	8.9×10^{-15}	98
IO + DMS	1.5×10^{-11}	1.0×10^{-15}	15000

kcal·mol^{-1}. The nonbonded I···H distance in the cis IO−DMS complex (3.356 Å) is larger than the sum of the vdW radii of iodine (2.16 Å)[33a] and hydrogen (1.10 Å)[33b] which may indicate little H-bonding. While the lowest orientation of the IO−DMS complex is trans, the cis OAT transition state (IO-OAT-TS-c) is 3.3 kcal·mol^{-1} lower in energy than the trans OAT (IO-OAT-TS-t C_1). Thus, the reaction path for the OAT reaction is predicted to start with IO in the trans orientation and reach the TS in the cis orientation which would suggest that the departing iodine radical should have significant angular motion.

The enthalpy of the OAT transition state is lower than the enthalpy of the IO−DMS complex (−1.3 compared to −2.6 kcal·mol^{-1}) which is not possible on a continuous PES but does occur when enthalpies are derived from a composite method such as G2B3(MP2). It should be noted that the free energy (298 K) of the OAT transition state, IO-OAT-TS-c, is 6.9 kcal·mol^{-1} higher than the free energy of IO + DMS, and the same free energy as the complex, IO−SMe_2-t C_1 (Table 3). Nakano et al.[10] have determined that the OAT reaction has a negative activation energy of −4.4 kcal·mol^{-1}.

The abstraction transition state is significantly higher in enthalpy than the OAT transition state (3.3 compared to −2.6 kcal·mol^{-1}). Since the bond enthalpy in the X−O bond should decrease in the order Cl−O > Br−O > I−O, it is expected that the OAT activation barrier should decrease in the same order. This expectation is fulfilled for the OAT activation enthalpies (1.3 > −0.4 > −2.6 kcal·mol^{-1} for ClO, BrO, and IO, respectively). On the other hand, the abstraction of hydrogen occurs from the oxygen end of XO and is not expected to change significantly (2.1, 2.0, and 3.3 kcal·mol^{-1} for ClO, BrO, and IO, respectively).

The OAT reaction enthalpy to form I + DMSO is calculated to be −38.3 kcal·mol^{-1} which is significantly more exothermic than the experimental value[17] of −29.0 kcal·mol^{-1}. It should be noted that the SOC of the I atom (which is included in the calculations) contributes 7.25 kcal·mol^{-1} to the exothermicity. The iodine radical is not expected to abstract a hydrogen from DMSO because the calculated bond enthalpy of HI (63.6 kcal·mol^{-1}) is much smaller than the calculated H−C bond enthalpy in DMSO (98.5 kcal·mol^{-1}). The abstraction pathway generates the HOI/$MeSCH_2$ complex which is bound by 5.1 kcal·mol^{-1} with respect to separated products.

The calculated rate constant[34] of the OAT pathway (1.5×10^{-11} $cm^3 \cdot s^{-1}$) is much faster than the abstraction pathway (1.0×10^{-15} $cm^3 \cdot s^{-1}$). While there is considerable disagreement among the experimental determinations of the rate constant (Table 1), the present calculations support a fast reaction between IO and DMS. A summary of the calculated rate constants is given in Table 4.

Bonding in XO−DMS Adducts. An estimate of the binding enthalpy of an unsymmetrical 2c−3e complex is given by the average of the symmetrical complexes times $e^{-\Delta IE}$ (eq 7), where ΔIE is the difference (measured in eV) in ionization energies, a factor related to "orbital matching".[35]

$$D_{AB} = ((D_{AA} + D_{BB})/2)e^{-\Delta IE} \quad (7)$$

TABLE 5: Experimental Binding Enthalpies (kcal·mol^{-1}) of X∴X$^-$, Calculated Binding Enthalpies (kcal·mol^{-1}) of XO∴OX$^-$, and Pseudo-IE (eV) of X$^-$ and XO$^-$

A	binding enthalpy of A∴A$^-$ [a]	exptl EA of A (eV)	work term (eV)[b]	pseudo-IE of A$^-$ (eV)
F	30.2	3.40	6.09	9.49
Cl	31.8	3.62	5.18	8.80
Br	27.9	3.36	4.52	7.88
I	24.3	3.06	4.12	7.18
OH	33.6[c]	1.84	6.09	7.93
OCl	20.6	2.27	4.12	6.39
OBr	21.4	2.35	4.12	6.47
OI	26.5	2.37	4.12	6.49

[a] The binding enthalpies of X∴X$^-$ (X = F, Cl, Br, I) are experimental values (see: Braïda, B.; Hiberty, P. C. *J. Phys. Chem. A* **2000**, *104*, 4618 and Chermette, H.; Ciofini, I.; Mariotti, F.; Daul, C. *J. Chem. Phys.* **2001**, *115*, 11068). The binding enthalpies (298 K) of XO∴OX$^-$ (X = H, Cl, Br, I) are calculated at the B3LYP/6-311+G(2df,p) level of theory. The IO∴OI$^-$ calculation used a basis set of similar size on iodine with an ECP replacing the core electrons. The assumed symmetry of the XO∴OX$^-$ complex was C_2 for X = H and Cl and C_{2h} for X = Br and I. The optimized O∴O distances in the XO∴OX$^-$ complexes were 2.419, 2.294, 3.517, and 3.428 Å for X = H, Cl, Br, and I, respectively. The calculated binding enthalpy (298 K) of $(DMS)_2^+$ at the B3LYP/6-31+G(d) level of theory is 29.8 kcal·mol^{-1}. Spin−orbital corrections are not included in the calculation of XO∴OX$^-$ binding enthalpies. [b] Work necessary to separate unit charges (work = $qQ/4\pi\epsilon_o R$) where R is assigned a reasonable value (Wine, P. H.; McKee, M. L. to be published). This term is added to the EA of A to give the pseudo-IE of the anion (A$^-$). A comparison of the pseudo-IE of A$^-$ and the IE of DMS (exptl 8.69 eV) will give an indication of orbital matching. A better orbital match between A$^-$ and DMS will lead to a stronger 2c−3e interaction. [c] The 2c−3e structure of HO∴OH$^-$ is known to collapse to lower-energy structures. See: Braïda, B.; Thogersen, L.; Hiberty, P. C. *J. Am. Chem. Soc.* **2002**, *124*, 11781.

An adjustment must be made for the ionization energy of XO$^-$ to take into account that a work term for separating charge is "missing" (Table 5). If the pseudo-IE of XO$^-$ is used rather than the EA (Table 5), then an estimate of orbital matching can be made. With the use of the pseudo-IE from Table 5, the orbital match for HO−DMS (ΔIE = 0.76 = 8.69−7.93, eV) is much better than the orbital match for ClO−DMS (ΔIE = 2.30 = 8.69−6.39, eV) which leads to a much greater predicted binding enthalpy for HO−DMS (eq 7, 14.8 kcal·mol^{-1})[36] compared to ClO−DMS (eq 7, 2.5 kcal·mol^{-1}). The corresponding estimates of the BrO−DMS and IO−DMS binding enthalpies from eq 7 are also small, 2.8 and 3.1 kcal·mol^{-1}, respectively. Thus, the ClO, BrO, and IO radicals are qualitatively different from OH in that the orbital match with DMS is poorer which leads to much smaller binding enthalpies. The calculated DFT binding enthalpies for XO−DMS (6.7, 6.1, and 7.8 kcal·mol^{-1} for ClO−DMS, BrO−DMS, and IO−DMS, respectively) are substantially larger than the G3B3, G3B3-(MP2), and G2B3(MP2) values (Table 3) due to known deficiencies in the DFT method for describing theses systems.[37]

The bonding between ClO and DMS in the ClO−DMS complex, as determined by an NBO population analysis at the B3LYP/6-311+G(d,p) level,[38] consists of one σ bond occupied by a single β-spin electron. There are no corresponding α-spin electrons in S−O bonding or antibonding orbitals, rather two unpaired α-spin electrons reside in nonbonding (singly occupied lone pair) orbitals (Figure 7). The β-bond is polarized toward sulfur (61.9%, Table 6). Since DMS donates 0.34 electrons to ClO, a most consistent interpretation of the bonding in the ClO−DMS complex is the formation of a β-electron dative bond (Figure 7), i.e., a β-bond (ClO ← SMe_2). The interpretation of

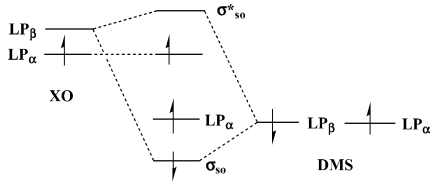

Figure 7. Interaction diagram of the singly occupied molecular orbital (SOMO) of XO (X = Cl, Br, I) interacting with the highest occupied molecular orbital (HOMO) of DMS.

TABLE 6: NPA Charges, Total Atomic Spin Densities, and β-Bond Polarization of the σ_{so} Bond in the XO−DMS Complex (X = Cl, Br, I)[a]

	NPA charge		spin densities		β-bond polarization	
	XO	DMS	O	S	O	S
ClO−SMe_2-c C_s	−0.34	0.34	0.54	0.37	38.1%	61.9%
BrO−SMe_2-t C_1	−0.36	0.36	0.54	0.38	39.7%	60.3%
IO−SMe_2-t C_1	−0.40	0.40	0.54	0.41	41.9%	58.1%

[a] At the B3LYP/6-311+G(d,p) for X = Cl and Br and at the B3LYP/6-311+G(d,p)/ECP level for X = I.

the XO−DMS bonding for X = Br and I is very similar to that for ClO−DMS.

Conclusions

The reaction rates between XO and DMS were computed for the oxygen-atom transfer (OAT) and hydrogen abstraction pathways. The relative reactivity of XO toward DMS is IO > BrO > ClO at 298 K and 760 Torr with rate constants of 3.0×10^{-15} $cm^3 \cdot s^{-1}$, 8.7×10^{-13} $cm^3 \cdot s^{-1}$, and 1.5×10^{-11} $cm^3 \cdot s^{-1}$ for ClO, BrO, and IO, respectively, at 298 K and 760 Torr. The abstraction pathway is less favored with calculated branching ratios of 2.7, 98, and 15 000 for ClO, BrO, and IO, respectively. The calculated rate constants for ClO and BrO with DMS are in good agreement with experiment, while the calculated rate constant for the IO plus DMS reaction overlaps at the "fast" end of experimental results. The binding enthalpies for ClO−DMS, BrO−DMS, and IO−DMS complexes (2.0, 1.7, and 1.3 kcal·mol^{-1}, respectively) are much weaker than the HO−DMS complex (13 ± 3 kcal·mol^{-1}) due to a poorer orbital match between XO and DMS (compared to OH and DMS).

Acknowledgment. Computer time was made available on the Alabama Supercomputer Network and the Auburn COSAM PRISM cluster. We thank Mr. Yongman Choi from Emory University for advice concerning the CHEMRATE program and Mr. Hyun Joo and Dr. Jimmy Mills for helpful conservations.

Supporting Information Available: B3LYP/6-311+G(d,p), G2B3(MP2), G3B3(MP2), and G3B3 energies (hartrees), zero-point energies (kcal·mol^{-1}), heat capacity corrections to 298 K (kcal·mol^{-1}), and entropies (cal·mol^{-1}·K^{-1}) (at the B3LYP/6-311+G(d,p) level) are tabulated in Table S1 (2 pages); a comparison of Br-containing species at the G2B3(MP2) and G3B3(MP2) levels is made in Table S2 (1 page); cartesian coordinates of all optimized structures in Table 3 at the B3LYP/6-311+G(d,p) level for Cl- and Br-containing species and at the B3LYP/6-311+G(d,p)/ECP level for I-containing species are given in Table S3 (11 pages). This material is available free of charge via the Internet at http://pubs.acs.org.

References and Notes

(1) Charlson, R. J.; Lovelock, J. E.; Andreae, M. O.; Warren, S. G. *Nature* **1987**, *326*, 655.

(2) Barone, S. B.; Turnipseed, A. A.; Ravishankara, A. R. *J. Chem. Soc., Faraday Trans.* **1995**, *100*, 39.

(3) Tyndall, G.; Ravishankara, A. R. *Int. J. Chem. Kinet.* **1991**, *23*, 483.

(4) Yin, F.; Grosjean, D.; Seinfeld, J. H. *J. Atmos. Chem.* **1990**, *11*, 309.

(5) Barnes, I.; Becker, K. H.; Martin, D.; Carlier, P.; Mouvier, G.; Jourdan, J. L.; Laverdet, G.; Le Bras, G. Impact of Halogen Oxides on Dimethyl Sulfide Oxidation in the Marine Atmosphere. In *Biogenic Sulfur in the Enviroment*; Saltzman, E. S., Cooper, W. J., Eds.; ACS Symposium Series 393; American Chemical Society: Washington, DC, 1989; p 464.

(6) Barnes, I.; Bastian, V.; Becker, K. H.; Overath, R. D. *Int. J. Chem. Kinet.* **1991**, *23*, 579.

(7) Díaz-de-Mera, Y.; Aranda, A.; Rodríguez, D.; López, R.; Cabañas, B.; Martínez, E. *J. Phys. Chem. A* **2002**, *106*, 8627.

(8) Bedjanian, Y.; Poulet, G.; Le Bras, G. *Int. J. Chem. Kinet.* **1996**, *28*, 383.

(9) Ingham, T.; Bauer, D.; Sander, R.; Crutzen, P. J.; Crowley, J. N. *J. Phys. Chem. A* **1999**, *103*, 7199.

(10) Nakano, Y.; Goto, M.; Hashimoto, S.; Kawasaki, M.; Wallington, T. J. *J. Phys. Chem. A* **2001**, *105*, 11045.

(11) Barnes, I.; Becker, H. K.; Carlier, P.; Mouvier, G. *Int. J. Chem. Kinet.* **1987**, *19*, 489.

(12) Martin, D.; Jourdain, J. L.; Laverdet, G.; Le Bras, G. *Int. J. Chem. Kinet.* **1987**, *19*, 503.

(13) Daykin, P. E.; Wine, P. H. *J. Geophys. Res.* **1990**, *95*, 18547.

(14) Maguin, F.; Mellouki, A.; Laverdet, G.; Poulet, G.; Le Bras, G. *Int. J. Chem. Kinet.* **1991**, *23*, 237.

(15) Knight, G. P.; Crowley, J. N. *Phys. Chem. Chem. Phys.* **2001**, *3*, 393.

(16) Nakano, Y.; Enami, S.; Nakamichi, S.; Aloisio, S.; Hashimoto, S.; Kawasaki, M. *J. Phys. Chem. A* **2003**, *107*, 6381.

(17) The webbook (http://webbook.nist.gov/chemistry) was used as the source of all thermochemistry except for the heat of formation of BrO and IO. BrO: (a) Bedjanian, Y.; Le Bras, G.; Poulet, G. *Chem. Phys. Lett.* **1997**, *266*, 233. IO: (b) Bedjanian, Y.; Le Bras, G.; Poulet, G. *J. Phys. Chem.* **1996**, *100*, 15130.

(18) Frisch, M. J.; Trucks, G. W.; Schlegel, H. B.; Scuseria, G. E.; Robb, M. A.; Cheeseman, J. R.; Zakrzewski, V. G.; Montgomery, J. A., Jr.; Stratmann, R. E.; Burant, J. C.; Dapprich, S.; Millam, J. M.; Daniels, A. D.; Kudin, K. N.; Strain, M. C.; Farkas, O.; Tomasi, J.; Barone, V.; Cossi, M.; Cammi, R.; Mennucci, B.; Pomelli, C.; Adamo, C.; Clifford, S.; Ochterski, J.; Petersson, G. A.; Ayala, P. Y.; Cui, Q.; Morokuma, K.; Malick, D. K.; Rabuck, A. D.; Raghavachari, K.; Foresman, J. B.; Cioslowski, J.; Ortiz, J. V.; Stefanov, B. B.; Liu, G.; Liashenko, A.; Piskorz, P.; Komaromi, I.; Gomperts, R.; Martin, R. L.; Fox, D. J.; Keith, T.; Al-Laham, M. A.; Peng, C. Y.; Nanayakkara, A.; Gonzalez, C.; Challacombe, M.; Gill, P. M. W.; Johnson, B. G.; Chen, W.; Wong, M. W.; Andres, J. L.; Head-Gordon, M.; Replogle, E. S.; Pople, J. A. *Gaussian 98*, revision A.11; Gaussian, Inc.: Pittsburgh, PA, 1998.

(19) Schaftenaar, G.; Noordik, J. H. MOLDEN. *J. Comput.-Aided Mol. Design* **2000**, *14*, 123.

(20) Curtiss, L. A.; Raghavachari, K.; Redfern, P. C.; Rassolov, V.; Pople, J. A. *J. Chem. Phys.* **1998**, *109*, 7764.

(21) Curtiss, L. A.; Raghavachari, K.; Pople, J. A. *J. Chem. Phys.* **1993**, *98*, 1293.

(22) Glukhovtsev, M. N.; Pross, A.; McGrath, M. P.; Radom, L. *J. Chem. Phys.* **1995**, *103*, 1878; erratum: **1996**, *104*, 3407.

(23) Curtiss, L. A.; Redfern, P. C.; Raghavachari, K.; Rassolov, V.; Pople, J. A. *J. Chem. Phys.* **1999**, *110*, 4703.

(24) Curtiss, L. A.; Redfern, P. C.; Rassolov, V.; Kedziora, G.; Pople, J. A. *J. Chem. Phys.* **2001**, *114*, 9287.

(25) (a) Schwerdtfeger, P.; Dolg, M.; Schwarz, W. H.; Bowmaker, G. A.; Boyd, P. D. W. *J. Chem. Phys.* **1989**, *91*, 1762. (b) Bergner, A.; Dolg, M.; Küchle, W.; Stoll, H.; Preuss, H. *Mol. Phys.* **1993**, *80*, 1431.

(26) (a) Furlani, T. R.; King, H. F. *J. Chem. Phys.* **1985**, *82*, 5577. (b) King, H. F.; Furlani, T. R. *J. Comput. Chem.* **1988**, *9*, 771. (c) Fedorov, D. G.; Gordon, M. S. *J. Chem. Phys.* **2000**, *112*, 5611.

(27) Stevens, J. E.; Cui, Q.; Morokuma, K. *J. Chem. Phys.* **1998**, *108*, 1554.

(28) Mokrushin, V.; Tsang, W. *CHEMRATE. A Calculational Data Base for Unimolecular Reactions*; National Institute of Standards and Technology: Gaithersburg, MD, 2000.

(29) (a) Glendening, E. D.; Reed, A. E.; Carpenter, J. E.; Weinhold, F. *NBO*, version 3.1. (b) Reed, A. E.; Curtiss, L. A.; Weinhold, F. *Chem. Rev.* **1988**, *88*, 899.

(30) Vandresen, S.; Resende, S. M. *J. Phys. Chem. A* **2004**, *108*, 2248.

(31) Stickel, R. E.; Nicovich, J. M.; Wang, S.; Zhao, Z.; Wine, P. H. *J. Phys. Chem.* **1992**, *96*, 9875.

(32) Butkovskaya, N. I.; Poulet, G.; Le Bras, G. *J. Phys. Chem.* **1995**, *99*, 4536.

(33) (a) Batsanov, S. S. *J. Chem. Soc., Dalton Trans.* **1998**, 1541. (b) Mandal, P. K.; Arunan, E. *J. Chem. Phys.* **2001**, *114*, 3880.

(34) Due to a limitation of the CHEMRATE program, we could not use a negative activation barrier. Therefore, we assumed an activation barrier as zero and multiplied the rate by $e^{-\Delta H/RT}$ where ΔH is the activation enthalpy (i.e $\Delta H_a = -0.4$ or $\Delta H_a = -2.6$ kcal·mol^{-1} for the OAT reaction of BrO and IO with DMS, respectively).

(35) Clark, T. *J. Am. Chem. Soc.* **1988**, *110*, 1672.

(36) The experimental binding enthalpy is 13.0 kcal·mol^{-1}: (a) Hynes, A. J.; Stoker, R. B.; Pounds, A. J.; McKay, T.; Bradshaw, J. D.; Nicovich, J. M.; Wine, P. H. *J. Phys. Chem.* **1995**, *99*, 16967. The calculated binding entrhalpy is 9−10 kcal·mol^{-1}. (b) Tureček, F. *Collect. Czech. Chem. Commun.* **2000**, *65*, 455. (c) Wang, L.; Zhang, J. *THEOCHEM* **2001**, *543*, 167. (d) McKee, M. L. *J. Phys. Chem. A* **2003**, *107*, 6819.

(37) For a summary of deficiencies of the DFT methods for describing 2c−3e systems see: (a) Gräfenstein, J.; Kraka, E.; Cremer, D. *Phys. Chem. Chem. Phys.* **2004**, *6*, 1096. (b) Fourré, I.; Bergès, J. *J. Phys. Chem. A* **2004**, *108*, 898.

(38) A NBO analysis at the MP2/6-311G(d,p) level (with the MP2 density matrix, i.e., DENSITY = CURRENT) gives a very similar description of the bonding for the ClO−DMS complex.